Exploiting Intelligent Reflecting Surface for Wireless Power Transfer via Optimization and Deep Learning Approaches

Pham Viet Tuan[1], **Vinh Anh Nghiem Quan**[1], **Pham Ngoc Son**[2], **Sang Quang Nguyen**[3], and **Pham Viet Hung**[4†], Non-members

ABSTRACT

In this paper, the wireless power transfer system with intelligent reflecting surface (IRS) assistance is studied to maximize the total harvested power at multiple users. The near optimal IRS phase shifts are obtained by two methods of successive convex approximation (SCA) and deep learning techniques. In the optimization method (IRS-OPT), we combine SCA technique with semidefinite relaxation to find the suboptimal solution with high harvested power performance. In the deep learning method (IRS-DL), the deep neutral network is proposed to learn the harvested power maximization via channel information. The numerical evaluations show that the IRS-OPT achieves the higher result while the IRS-DL provides the solution with almost real-time computation.

Keywords: Wireless Power Transfer, Intelligent Reflecting Surface, Successive Convex Approximation, Deep Learning, Semidefinite Relaxation

1. INTRODUCTION

Many different sectors of our society such as healthcare, manufacturing, transportation, smart home, etc., have applications of Internet-of-Things (IoT) devices where the limited amount of energy in device batteries is the bottleneck of the performances of wireless systems. Moreover, the energy starving of the battery-powered wireless devices such as low-power physical devices (e.g., sensor, actuators, internet-of-things) is a crucial problem [1–7]. To address this issue, the wireless power transfer (WPT) with a power beacon is a promising approach to provide controllable energy instead of the unstable natural energy. In addition, the WPT systems eliminate the high cost of battery replacement and enable far-field wireless energy transmission, enlarge the near-field wireless charging distance, and prolong the lifetimes of wireless devices. However, the severe degradation of wireless signal via the long distance is a main limited of the wireless power transfer.

Recently, there is a promising technology, namely intelligent reflecting surface (IRS), to achieve high energy efficiency with low power consumption and hardware cost [8–13] where IRS utilizes the vast low-cost passive reflecting elements integrated on a planar surface. In general, an IRS element can independently adjust the phase of reflected signal to smartly configure favorable wireless propagation channels. Then, the reflected signals can be steered to the desired receivers to enhance the power of received signals. Specifically, we investigate the design of IRS phase shifts to enhance the total harvested energy for wireless power transfer.

1.1 Related Works

In [14], the authors investigated the weighted sum harvested power with semidefinite relaxation (SDR) method for finding the optimal phase shifts. However, the Gaussian relaxation method is applied to obtain the approximate suboptimal solution when the rank-1 condition is not satisfied. In [15], the achievable data rate was maximized in simultaneous wireless information and power transfer multiple-input multiple-output (MIMO) system with IRS assistance. In [16], the wireless power transfer was used to provide energy for sensors, then the sensors collaborate to send information to the access point (AP). The sensing and energy consumption of sensors was considered and the signal-to-noise ratio (SNR) at the AP was maximized. However, the IRS have not applied to enhance the power transfer efficiency.

In [17], the energy beamforming and over-the-air computation were combined to minimize the mean square error of uplink message in IRS-aided IoT networks. In [18], the waveform of signal and passive beamforming were combined to maximize energy transmission for a group of users. However, the Gaussian randomization was used to obtain the passive beamforming vector. In [19], the author studied the IRS-assisted wireless powered communication where the

Manuscript received on December 1, 2022; revised on April 21, 2023; accepted on June 7, 2023. This paper was recommended by Associate Editor Suramate Chalermwisutkul.

[1]The authors are withUniversity of Education, Hue University, Thua Thien Hue, Vietnam.

[2]The author is with Ho Chi Minh City University of Technology and Education, Ho Chi Minh City, Vietnam.

[3]The author is with Science and Technology Application for Sustainable Development Research Group, Ho Chi Minh City University of Transport, Ho Chi Minh City, Vietnam.

[4]The author is with Vietnam Maritime University, Hai Phong, Vietnam.

[†]Corresponding author: phamviethung@vimaru.edu.vn

Digital Object Identifier: 10.37936/ecti-eec.2023213.251465

users harvested radio frequency energy and then sent the information back to the base station. The time allocation and passive IRS beamforming were optimized via the target of user sum-rate maximization.

The drawbacks of the conventional optimization approach is to require the iterative convex solution that makes high complexity and limited practical applications. The recent detonation of successful performance of machine learning in wireless communication and optimization have received much of attention in both academic and industrial [20–23]. In approaches based on deep learning, the fast computation in comparison with the conventional iterative non-convex optimization procedure is a remarkable benefit in real-time applications. In [24], the authors exploited deep learning in phase configuration for single user multi-input single-output system with IRS aid. The deep neutral network was trained by the received pilot signal as input data, phase shifts at IRS and beamforming vector at the base station as output data. In [25], the receiver's location and attributes were used to train deep neutral network to maximize data rate and obtain the optimal IRS phase shifts instead of the estimated channels or the pilot signals. We note that the mentioned works utilized supervised learning method with large data labels generated by the conventional optimization algorithm. In [26], the hybrid beamforming with the analog part is assigned by the deep neutral network method for multiple users. The aim is to maximize the sum data rate of all users with unsupervised learning method. To reduce the overhead of training data generation, the authors in [27] constructed a DNN to achieve the data rate maximization for single user IRS-aided system where the input data is the estimated channel information.

1.2 Main Contributions

In this study, we investigate the WPT system where the power beacon sends the signals reflected by the IRS to the multiple users. In the considered WPT system, the wireless energy signal is severely degraded by blockage, the IRS can concentrate the energy signals to the users by surpassing obstacles. Hence, the energy harvesting performance is guaranteed even in non-light-of-sight transmission when the IRS design is optimized. As a result, this work can enhance the wireless power transfer efficiency with IRS support in high attenuation environment. The target is to maximize the total harvested power of all users by optimizing the IRS phase shifts. A comparative investigation of two approaches based on the optimization and deep learning techniques is performed for the IRS-aided wireless power transfer system with multiple users. The main contributions are described as follows.

- The IRS-aided WPT system with multiple harvested energy users is considered for the target of total harvested power maximization. The optimal phase shifts is obtained by the first IRS-OPT algorithm where the rank-1 approximation is solved by the successive convex approximation (SCA) and exact penalty function method.
- The second IRS-DL approach is proposed via deep neutral network where the loss function is formulated by the total harvested power and the optimal phase shifts are obtained at the last hidden layer. In addition, the deep learning network is trained by the input data of processing channel information and loss function via a unsupervising method.
- The numerical results present the convergences of IRS-OPT and IRS-DL methods. Also, the IRS-OPT method provides the better harvested power for users than the IRS-DL method does. In contrast, the IRS-DL approach obtains results almost real time computation compared to the IRS-OPT algorithm.

***Table 1**: Main symbols*

Symbols	Meanings
N	Number of IRS elements
K	Number of users
$\mathbf{g}$	Channel vector from PB to IRS
$\mathbf{h}_k$	Channel vector from IRS to k-th user
P	Transmission power at PB
$\boldsymbol{\Psi}$	Phase shift matrix of IRS
η_k	Energy conversion efficiency at k-th user
φ_n	Phase shift at n-th element

The remain of this work is arranged as follows. Section 2 presents the system model and the problem formulation. In Section 3, the IRS-OPT approach is presented and summarized in Algorithm 1. In Section 4, we present the second IRS-DL approach where the deep neutral network architecture, the loss function, and the input/output layers are in details. Finally, Section 5 presents the numerical results, followed by the conclusion in Section 6.

Notations. Vectors and matrices are indicated by boldface uppercase and lowercase letters, respectively. $\mathbf{X}^H$, $\mathrm{Tr}(\mathbf{X})$, and $\mathrm{rank}(\mathbf{X})$ are used for the conjugate transpose, trace, and rank of matrix $\mathbf{X}$, respectively. We denote $\mathbf{X} \succeq 0$ for positive semidefinite matrix. By $\|\mathbf{x}\|$ and $|x|$, the norm-2 of a complex vector $\mathbf{x}$ and the absolute value of a complex scalar x are represented, respectively. We also denote $\mathbb{C}^{m\times n}$ for the space of $m \times n$ complex matrices.

2. SYSTEM MODEL

In this part, we introduce the multi-user wireless power transfer system with the aid of IRS and formulate the optimization problem of IRS shift-phase design. The main symbols and their meanings are presented in Table 1.

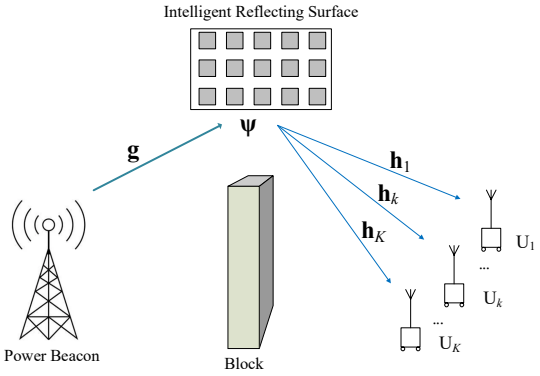

***Fig. 1**: IRS-aided wireless power transfer system.*

2.1 IRS-Aided WPT System

As shown in Fig. 1, the IRS-aided wireless power transfer system includes one power beacon (PB), one IRS supporting the energy transfer, and multiple energy harvesting users. The IRS is integrated in wireless powered communication system as [37, 38] with many IoT applications for smart home, smart city and wireless sensor network. The IRS is equipped by N reflecting elements, and K single-antenna users harvest energy from the PB. Since the direct links from the PB to EH users are assumed to be blocked by the obstacles in the considered scenario, thus the IRS has the key role to reflect the energy signal to the energy harvesting (EH) users.

We denote the PB-IRS and IRS-kth user channels as $\mathbf{g} \in \mathbb{C}^{N\times 1}$, $\mathbf{h}_k \in \mathbb{C}^{N\times 1}$, respectively. The phase-shift matrix at the IRS is denoted by $\boldsymbol{\Psi} = diag\left(\left[e^{j\varphi_1}, e^{j\varphi_2}, ..., e^{j\varphi_N}\right]^T\right)$ where φ_n is the phase shift at the n-th IRS element, $n \in \{1, .., N\}$. To reflect maximum power of the incoming signal, the amplitude reflecting coefficients are assumed as 1, similar to [28, 29]. As a result, the received signal at the k-th user is expressed as

$$r_k = \mathbf{h}_k^H \boldsymbol{\Psi} \mathbf{g}\left(\sqrt{P}x\right) + n_k, \forall k \in \{1, .., K\} \tag{1}$$

where x is signal symbol with $E\left\{|x|^2\right\} = 1$ and P is the transmit power at the PB. In addition, $n_k \sim \text{CN}\left(0, \sigma_k^2\right)$ denotes the additive white Gaussian noise (AWGN) at the k-th EH user. Then, the amount of harvested power at the k-th user is given as

$$\Phi_k = \eta_k E\left\{\left|r_k\right|^2\right\} = \eta_k P\left|\mathbf{h}_k^H \boldsymbol{\Psi} \mathbf{g}\right|^2, \forall k, \tag{2}$$

where $\eta_k \in (0, 1]$ is energy conversion efficiency for harvesting power at the k-th user. We note that the noise power is omitted since it is small in comparison to the harvested power amount of signals. Therefore, the total harvested power of all users is obtained as $\sum_{k=1}^{K} \eta_k P\left|\mathbf{h}_k^H \boldsymbol{\Psi} \mathbf{g}\right|^2$.

2.2 Problem Formulation

The aim of IRS-aided WPT system is to maximize the total harvested power of all users by optimizing the phase shifts of IRS elements. The energy harvesting maximization problem is to formulate as follows.

$$\max_{\{\varphi_n\}} \sum_{k=1}^{K} \eta_k P\left|\mathbf{h}_k^H \boldsymbol{\Psi} \mathbf{g}\right|^2 \tag{3a}$$

$$\text{s.t.: } \boldsymbol{\Psi} = diag\left(\left[e^{j\varphi_1}, e^{j\varphi_2}, ..., e^{j\varphi_N}\right]^T\right) \tag{3b}$$

$$\varphi_n \in [0, 2\pi), \forall n \tag{3c}$$

The objective function is the harvested power sum of K users while the constraint is the limit of phase shifts at the IRS. In this work, we proposed two approaches of optimization and deep learning for solving the considered IRS design problem. In the optimization method, the successive convex approximation is combined with the exact penalty function method to obtain the suboptimal solution. In the second method, the deep learning technique is exploited to find the almost real-time solution where the unsupervised training process for the deep neutral network uses the modified channels information.

3. OPTIMIZATION APPROACH FOR IRS DESIGN

In this section, we propose the solution via the conventional optimization method by utilizing SCA and penalty function methods instead of the Gaussian randomization method as [18, 40]. We first perform some manipulations to simplify the expression of the objective function as follows.

$$\begin{aligned} \mathbf{h}_k^H \boldsymbol{\Psi} \mathbf{g} &= \left[e^{j\varphi_1}, e^{j\varphi_2}, ..., e^{j\varphi_N}\right] \text{diag}\left(\mathbf{h}_k^H\right) \mathbf{g} \\ &= {}^H\text{diag}\left(\mathbf{h}_k^H\right) \mathbf{g} \end{aligned} \tag{4}$$

where $\mathbf{z} = \left[e^{-j\varphi_1}, e^{-j\varphi_2}, ..., e^{-j\varphi_N}\right]^T$. We denote $\mathbf{a}_k = \text{diag}\left(\mathbf{h}_k^H\right) \mathbf{g} \in \mathbb{C}^{N\times 1}$ and derive $\left|\mathbf{h}_k^H \boldsymbol{\Psi} \mathbf{g}\right|^2 = \left|\mathbf{z}^H \mathbf{a}_k\right|^2$. Thus, by applying $\text{Tr}(\mathbf{AB}) = \text{Tr}(\mathbf{BA})$ via [35], we obtain

$$\begin{aligned} \left|\mathbf{z}^H \mathbf{a}_k\right|^2 &= \left(\mathbf{z}^H \mathbf{a}_k\right)^H \left(\mathbf{z}^H \mathbf{a}_k\right) \\ &= \text{Tr}\left(\mathbf{a}_k^H \mathbf{z}\mathbf{z}^H \mathbf{a}_k\right) \\ &= \text{Tr}\left(\mathbf{a}_k \mathbf{a}_k^H \mathbf{z}\mathbf{z}^H\right) \end{aligned} \tag{5}$$

Moreover, by the SDR technique [30, 36] where the condition $\mathbf{Z} = \mathbf{z}\mathbf{z}^H$ is equivalent to $\mathbf{Z} \succeq 0$ and rank () = 1. We denote $\mathbf{A}_k = \mathbf{a}_k \mathbf{a}_k^H$ to achieve $\left|\mathbf{z}^H \mathbf{a}_k\right|^2 = \text{Tr}\left(\mathbf{A}_k \mathbf{Z}\right)$. Thus, we use the novel matrix variable $\mathbf{Z}$ and reformulate the optimization problem as follows.

$$\max_{\mathbf{Z}\in\mathbb{H}^N} P \sum_{k=1}^{K} \eta_k \text{Tr}\left(\mathbf{A}_k \mathbf{Z}\right) \tag{6a}$$

$$\text{s.t.: } [\mathbf{Z}]_{n,n} = 1, \forall n \tag{6b}$$

$$\mathbf{Z} \succeq 0 \tag{6c}$$

$$\text{rank}(\mathbf{Z}) = 1 \tag{6d}$$

We observe that the rank-1 constraint is non-convex and the positive semidifinite matrix $\mathbf{Z}$ satisfies $\mathrm{Tr}(\mathbf{Z}) \geq \lambda_1(\mathbf{Z})$ where $\lambda_1(\mathbf{Z})$ is the maximum eigenvalue of $\mathbf{Z}$ and every eigenvalues of $\mathbf{Z}$ is non-negative [35, 36]. Thus, the rank-1 constraint can be replaced by the new constraint $\mathrm{Tr}(\mathbf{Z}) - \lambda_1(\mathbf{Z}) \leq 0$. We next apply the exact penalty function method [31] to move the new constraint to the objective function and utilize the SCA method [34]. The problem (6) is rewritten as

$$\min_{\mathbf{Z}\in\mathbb{H}^N} \quad -P\sum_{k=1}^{K}\eta_k \mathrm{Tr}\left(\mathbf{A}_k\mathbf{Z}\right) + \mu\left(\mathrm{Tr}(\mathbf{Z}) - \lambda_1(\mathbf{Z})\right) \tag{7a}$$

$$\text{s.t.:} \quad [\mathbf{Z}]_{n,n} = 1, \forall n \tag{7b}$$

$$\mathbf{Z} \succeq 0 \tag{7c}$$

where the large parameter μ is a penalty factor which penalizes the positive value of $\left(\mathrm{Tr}(\mathbf{Z}) - \lambda_1(\mathbf{Z})\right)$. We exploit the iterative method of SCA to solve the non-convex optimization problem. We base on the inequation

$$\lambda_1(\mathbf{Z}) \geq \lambda_1\left(\mathbf{Z}^{(i)}\right) + \mathbf{v}_1^{(i)H}\left(\mathbf{Z} - \mathbf{Z}^{(i)}\right)\mathbf{v}_1^{(i)} \tag{8}$$

for two positive semidefinite matrices $\mathbf{Z}$, $\mathbf{Z}^{(i)}$, and the eigenvector according to $\lambda_1\left(\mathbf{Z}^{(i)}\right)$ via [34]. Then, we solve the subproblem with the fixed $\mathbf{Z}^{(i)}$ as follows:

$$\begin{aligned}\min_{\mathbf{Z}\in\mathbb{H}^N} \quad & -P\sum_{k=1}^{K}\eta_k \mathrm{Tr}\left(\mathbf{A}_k\mathbf{Z}\right) \\ & +\mu\left(\mathrm{Tr}(\mathbf{Z}) - \left(\lambda_1\left(\mathbf{Z}^{(i)}\right) + \mathbf{v}_1^{(i)H}\left(\mathbf{Z} - \mathbf{Z}^{(i)}\right)\mathbf{v}_1^{(i)}\right)\right)\end{aligned} \tag{9a}$$

$$\text{s.t.:} \quad [\mathbf{Z}]_{n,n} = 1, \forall n \tag{9b}$$

$$\succeq 0 \tag{9c}$$

The optimal solution $\mathbf{Z}^*$ of Problem (9) is used for updating the fixed $\mathbf{Z}^{(i)}$ in the next iteration. The iterative values of objective function is descent and convergent to a local optimal point of the non-convex optimization problem (6) with rank-1 constraint. The proof is similar to that in [34] and here we omit it. Lastly, the proposed algorithm 1 presents the optimization approach in details.

4. DEEP LEARNING APPROACH FOR IRS DESIGN

In recent years, machine learning techniques have witnessed multiple successes in other fields such as computer vision and natural language processing. A deep neural network (DNN) can serve as an alternative to the iterative IRS optimization process, as it can approximate the output of the optimization problem directly by learning the input. Furthermore, contrary to the higher computational complexity of the backpropagation process during the initial training stage, upon being deployed, its forward passes in the inference stage only involves simple arithmetic operations, thus offering this approach computational superiority over the iterative algorithm, rendering it viable for real-time use. In this work, the unsupervised learning and new loss function of the harvested power are exploited to find the IRS phase-shifts solution instead of the supervised learning with labeled data or different loss function of mean square error (MSE) as [22, 24, 28]. The second deep learning method achieves the near optimal phase shifts with the almost real-time solution.

Algorithm 1: Proposed IRS-OPT algorithm for optimizing IRS-aided wireless power transfer

Input: Accuracy value ε_{acc}, maximum iteration number $I_{\max}$, penalty factor μ.

Output: *, $\left\{\varphi_n^*\right\}$.

For $i = 1, ..., I_{\max}$ **do**
  Solve convex subproblem (9) by Matlab's CVX tool [32], thus obtain optimal solution $\mathbf{Z}^*$, $\lambda_1\left(\mathbf{Z}^*\right)$, $\mathbf{v}_1\left(\mathbf{Z}^*\right)$.
  If $\mathrm{Tr}\left(\mathbf{Z}^*\right) - \lambda_1\left(\mathbf{Z}^*\right) \leq \varepsilon_{acc}$ **do**
    Break for loop.
  End If
  Update $\mathbf{Z}^{(i+1)} \leftarrow \mathbf{Z}^*$, $\lambda_1\left(\mathbf{Z}^{(i+1)}\right) \leftarrow \lambda_1\left(\mathbf{Z}^*\right)$, $\mathbf{v}_1^{(i+1)} \leftarrow \mathbf{v}_1\left(\mathbf{Z}^*\right)$.
End For

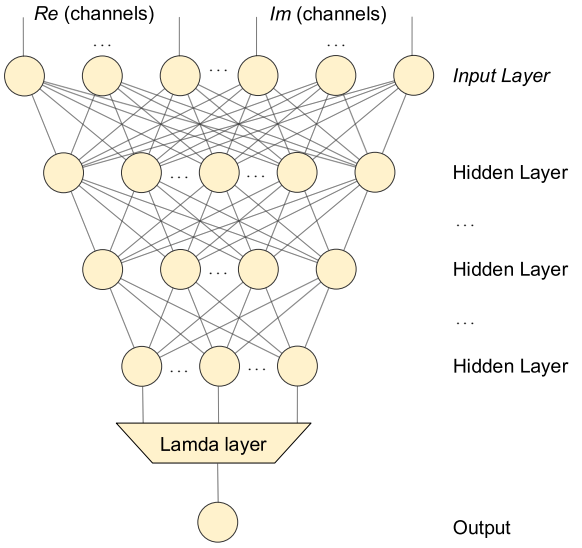

***Fig. 2**: Deep neutral network architecture.*

***Table 2**: DNN architecture parameters*

Layer	Output shape	Param.#
Input Layer	$[2N, 1]$	0
FC Layer 1	[512, 1]	$512 \times (2N + 1)$
FC Layer 2	[256, 1]	131,328
FC Layer 3	[128, 1]	32,896
FC Layer 4	[64, 1]	8,256
Lambda Layer	[64, 1]	0

4.1 Network Architecture

We implement our customized fully-connected DNN which consists of one input layer and four hidden layers as shown in Fig. 2. The output of each hidden layer can be expressed as:

$$\boldsymbol{\Sigma}_{\text{out}} = \mathbf{W}_0 + \mathbf{W}_1\mathbf{X}_1 + \mathbf{W}_2\mathbf{X}_2 + ... + \mathbf{W}_L\mathbf{X}_L \quad (10)$$

where $\mathbf{W}_0$ and $\mathbf{W}_i$ are the biases weights of the layer, and $\mathbf{X}_i$ is the output of the previous layer. Through the training process, our model will gradually correct its set of weights which allows it to obtain the optimal solution. A custom Lambda layer is put at the end of the last fully-connected layer. The Lambda layer's output provides the estimated phase shifts $\{\varphi_n\}$, then the Euler formula is applied to obtain the phase shift vector in complex form as

$$\begin{aligned}&\left[e^{j\varphi_1}, \ldots, e^{j\varphi_N}\right]\\ &= \left[\cos\left(\varphi_1\right) + j\sin\left(\varphi_1\right), \ldots, \cos\left(\varphi_N\right) + j\sin\left(\varphi_N\right)\right]\end{aligned} \quad (11)$$

Different from conventional DNNs which often use mean square error (MSE) as loss function to evaluate the accuracy of the labels of the predicted samples to that of training samples, we define a custom loss function directly related to the objective:

$$\begin{aligned}LF_{\text{THP}} &= -\frac{1}{T}\sum_{t=1}^{T}\sum_{k=1}^{K}\eta_k P\left|\mathbf{h}_k^H\boldsymbol{\Psi}\mathbf{g}\right|^2\\ &= -\frac{1}{T}\sum_{t=1}^{T}\sum_{k=1}^{K}\eta_k P\left|\left[e^{j\varphi_1}, \ldots, e^{j\varphi_N}\right]\left(\text{diag}\left(\mathbf{h}_k^H\right)\mathbf{g}\right)\right|^2\end{aligned} \quad (12)$$

where LF_{THP} denotes as the loss function of total harvested power at all users and T represents the number of training samples. This combined with the custom Lambda layer allows the IRS-DL model to output the total harvested power directly through the inference stage.

4.2 Hyperparameters

Hyperparameters in DNN context usually is a combination of the number of neurons, learning rate, batch size, activation function, optimization algorithm. The details of DNN architecture and parameters are presented in Table 2. Through empirical trials, we settle for the following configurations where the hidden layers are implemented with 512, 256, 128, 64 neurons, respectively. We tested a variety of different combinations of learning rate and batch size, and our simulations suggested that an initial learning rate 10^{-5} and a batch size of 128 offers the best in terms of convergence and performance. We utilize Adam [41] as optimization algorithm, as it offers faster convergence compared to stochastic gradient descent (SGD). Our training is performed on a training set consisting of 10^5 samples, in which 10^4 samples are reserved for validation. The well-known Adam optimization method provides the convergence of loss function values in training stage. We test our model on a testing set of 200 samples to obtain the final result.

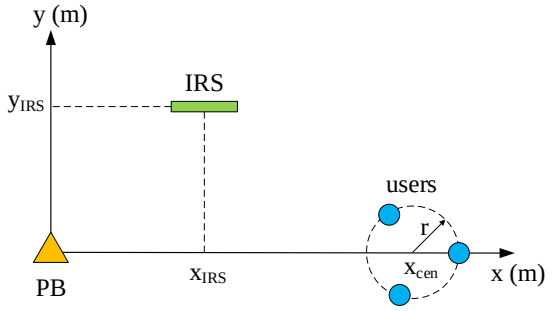

***Fig. 3**: System setup in the simulation.*

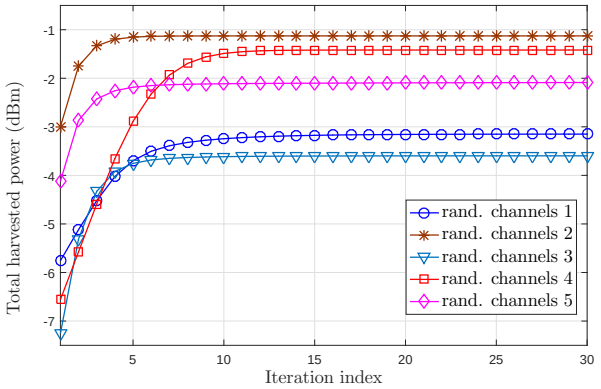

***Fig. 4**: Convergence behaviour of proposed algorithm 1 for the number of IRS elements, $N = 8$.*

5. SIMULATION RESULTS

In this section, the numerical results of the proposed IRS-OPT and IRS-DL approaches are presented to show the effectiveness of proposed solutions. The schematic network model for IRS-aided WPT design is plotted in Fig. 3. The positions of PB and IRS are $(0, 0)$ and $(x_{\text{IRS}}, y_{\text{IRS}})$ where $x_{\text{IRS}} = 5\,\text{m}$, $y_{\text{IRS}} = 3\,\text{m}$, unless otherwise stated. Moreover, the users' positions are uniformly distributed in the circle with the center point $(x_{\text{cen}} = 10\,\text{m}, 0\,\text{m})$ and the radius $r = 0.5\,\text{m}$. The channels include the large-scale path loss and small-scale Rayleigh fading. The path-loss exponents of the channels between the PB and the IRS, between the IRS and the users are 2.2, similar to [33]. The transmission power at the PB is $P = 40\,\text{dBW}$, the accuracy factor $\epsilon_{acc} = 10^{-5}$, and the penalty factor $\mu = 10^2$.

The simulations of both method are realized on a system configured with a Core i5-8400 and 8GB of RAM. We use Tensorflow library version 2.0, Python 3.7 and Matlab R2016a.

5.1 IRS-OPT Algorithm Results

The convergence behavior of the IRS-OPT algorithm with $N = 8$ is shown in Fig. 4. It can be seen that the total harvested power of users increases and converges within 30 iterations for different channel realizations. Thus, we

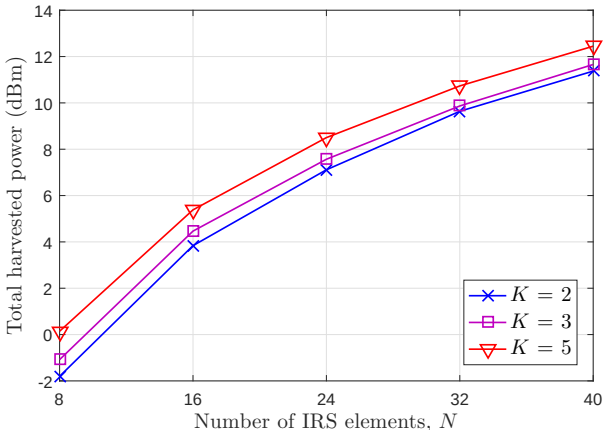

***Fig. 5**: Total harvested power versus number of IRS elements, N.*

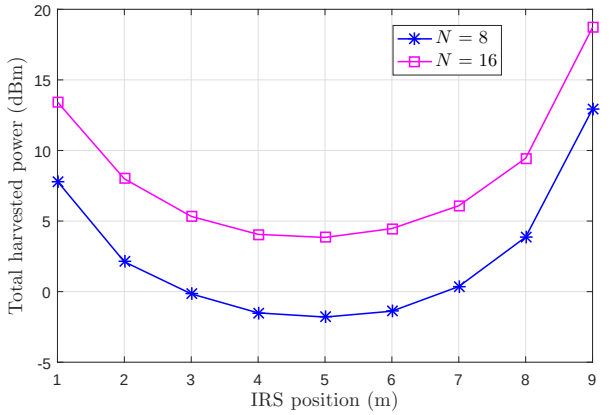

***Fig. 6**: Total harvested power versus IRS position, x_{IRS}.*

set the maximum iteration number $I_{\max} = 30$ for the convergent guarantee in the simulation.

Fig. 5 illustrates the total harvested power of all users versus the number of IRS elements when the number of users $K = 2, 3, 5$. It can be observed that the amount of harvested power rises as increasing the element number N. For example, when $K = 3$, the results are 4.47 dBm, 9.87 dBm with $N = 16, 32$, respectively. The reason is that the IRS can focus the reflecting signal to the users better when having more reflecting elements. Moreover, we can exploit the larger degree of freedom of a variable number in IRS phase-shift vectors to achieve higher objective value of harvested energy in Problem (3). In addition, the greater number of users harvests more energy in the case of the same IRS element number.

Fig. 6 presents the total harvested power versus IRS position where x_{IRS} is adjusted from the PB to the centre point of user circle and y_{IRS} is fixed for $N = 8, 16$. It can be observed in Fig. 6, the IRS position achieves the low performance in the middle of the PB and the devices, and the high power in the short distance from the PB or the devices. The reason is that the signal attenuation is high when the IRS is around of the middle and vice versus. Nevertheless, the investigation of the IRS deployment

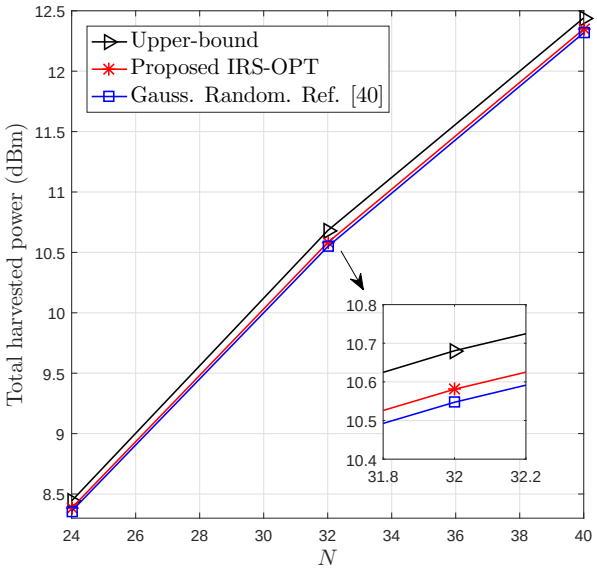

***Fig. 7**: Total harvested power versus number of IRS elements, N.*

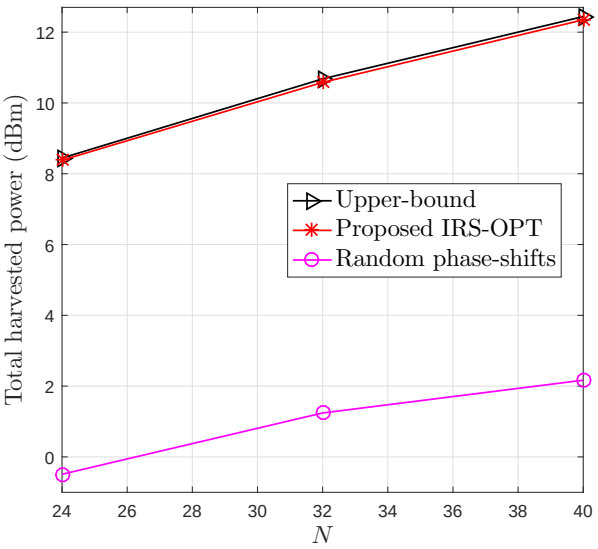

***Fig. 8**: Total harvested power versus number of IRS elements, N.*

still needs to choose the IRS coordinate in future works.

For comparison, the Gaussian randomization, upper-bound, and random phase-shifts approaches are presented as follows. First, the Gaussian randomization in [40] is performed to obtain the approximate phase-shift vector as follows. The problem (6) without rank-1 constraint is solved by CVX to obtain optimal solution, $\mathbf{Z}^*$. When $\text{rank}\left(\mathbf{Z}^*\right) > 1$, the eigendecomposition of $\mathbf{Z}^*$ is performed as $\mathbf{Z}^* = \mathbf{V}\Lambda\mathbf{V}^H$ where $\mathbf{V} \in \mathbb{C}^{N\times N}$ is a unitary matrix where the column vectors are the eigenvectors corresponding to the eigenvalues in the diagonal matrix $\boldsymbol{\Lambda} \in \mathbb{C}^{N\times N}$. We repeat I_{GR} iterations for generating the vector $\tilde{\mathbf{z}} = \mathbf{V}\boldsymbol{\Lambda}^{1/2}\mathbf{w}$ where $\mathbf{w}$ is a circularly symmetric complex Gaussian distribution random

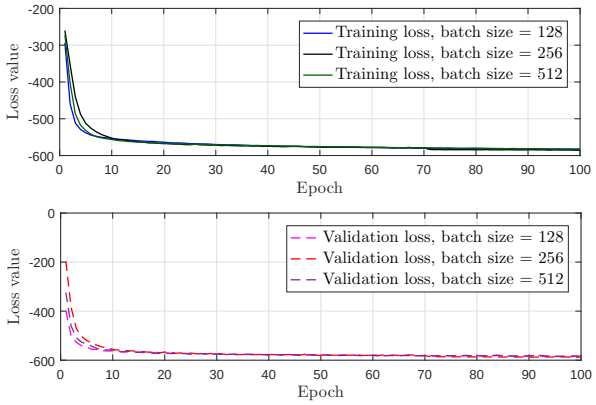

***Fig. 9**: Training and validation losses for 10^5 data samples of channel realizations with $N = 8$, $K = 2$.*

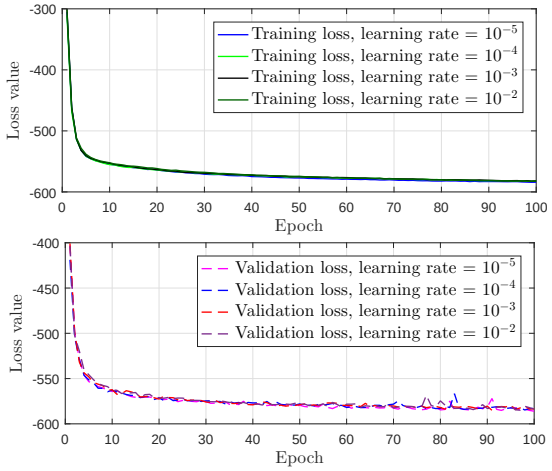

***Fig. 10**: Training and validation losses for 10^5 data samples of channel realizations with different learning rates.*

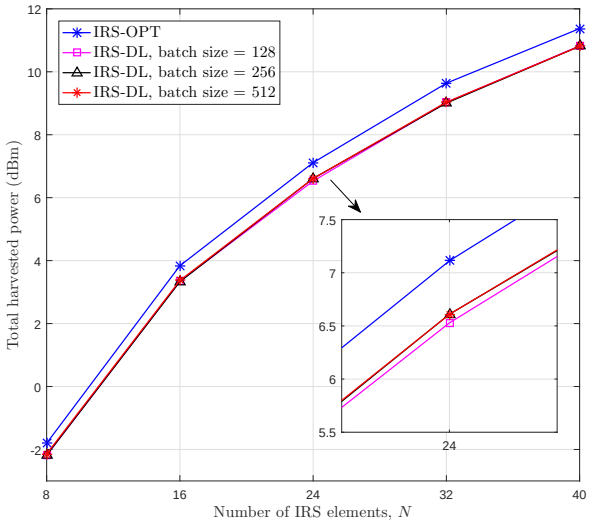

***Fig. 11**: Total harvested power versus number of IRS elements, N.*

vector, $\mathbf{w} \sim \mathrm{CN}\left(0, \mathbf{I}_N\right)$. Then, we derive the candidate vector $\mathbf{z} = e^{j \arg(\tilde{\mathbf{z}})}$, and thus the total harvested power at EH users is achieved for each iteration. The phase-shifts $\left\{\varphi_n^*\right\}$ with the best harvested power value is selected in I_{GR} iterations. Second, in the baseline of upper-bound, the value is obtained by solving Problem (6) without rank-1 constraint while in the second baseline, the phase-shifts at the IRS are assigned by random values in $[0, 2\pi)$.

The simulation results of the different methods are presented for comparison in Figs. 7 and 8. In Fig. 7, when the rank of optimal solution of Problem (6) without rank-1 constraint is larger than 1, the proposed IRS-OPT achieves the better harvested power in comparison to Gaussian randomization method while the upper-bound case gives the highest values. The reason is that the rank-1 constraint does not need to satisfy in the upper-bound case. Moreover, the IRS-OPT provides the approximate solution of rank-1 phase-shift matrix. In Fig. 8, the IRS-OPT also achieves the much higher harvested power than that of the random phase-shifts since when the phase-shifts are optimized in IRS-OPT method.

5.2 IRS-Deep Learning Method Results

The effect of different batch sizes on the training loss of our IRS-DL model can be observed in Fig. 9. We notice that with a batch size of 128, the training loss value decreases faster initially but all three batch size configurations in our simulations converge identically after about 10 epochs. A similar trend was observed with validation losses. The difference is even less negligible in Fig. 10, where we test different initial learning rate configurations.

As illustrated in Fig. 11, the simulation results of different batch size configurations for our IRS-DL method are identical and closely match the performance of the IRS-OPT method. The harvested power value also increases correspondingly to the number of IRS elements. We attribute this insensitivity of our network performance towards its hyper-parameters to our choice of network architecture and our simulation dataset of 10^5 samples. The combination of an appropriate network design with a relatively large dataset allow us to minimize the need of hyper-parameter tuning.

As for the inference time, i.e. the time required to predict the harvested power value of an input sample, is shown in Fig. 12. It can be observed that our IRS-DL model can offer approximate performance to the IRS-OPT method, while consuming order of magnitude less amount of time.

It should be noted that the training time of the IRS-DL approach is not included, as the training phase itself is realized during the offline stage of the network, and does not affect the inference stage which is realized entirely online afterwards once the network has been deployed. The performance of our IRS-DL approach combined with its modest computation time suggests that it can be applied in real-time scenarios.

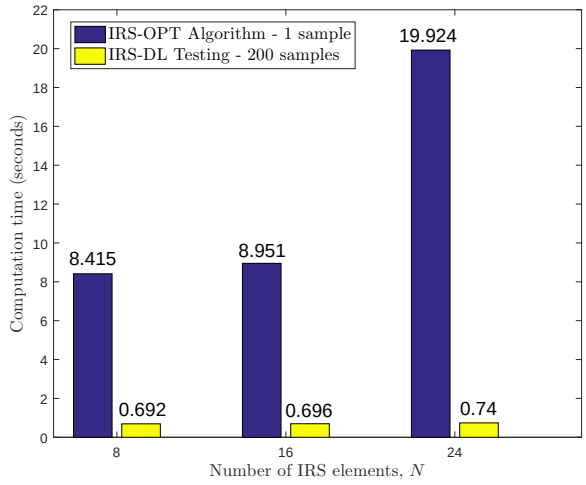

***Fig. 12**: Computation time.*

6. CONCLUSION

In the considered IRS-aided wireless energy transfer system, the harvested energy of all users is maximized by configuring the optimal IRS phase shifts under the two approaches of optimization and deep learning methods. The fast convergences of IRS-OPT and IRS-DL approaches to obtain the optimal points are shown in numerical simulations. In addition, the Gaussian randomization, upper-bound and random phase-shifts methods are performed in comparison to the proposed approaches. The IRS-OPT method provides better performance in terms of total harvested energy while the IRS-DL method enable to obtain almost real-time phase shift design. Finally, the extensions of the proposed works with multiple transmit antennas at the PB and the imperfect channel information are valuable to investigate in the future.

ACKNOWLEDGMENT

This work was supported by Hue University under the Core Research Program, Grant No. NCM.DHH.2022.08.

REFERENCES

[1] S. Bi, C. K. Ho, and R. Zhang, "Wireless powered communication: opportunities and challenges," *IEEE Communications Magazine*, vol. 53, no. 4, pp. 117–125, Apr. 2015.

[2] Y. Alsaba, S. K. A. Rahim, and C. Y. Leow, "Beamforming in Wireless Energy Harvesting Communications Systems: A Survey," *IEEE Communications Surveys & Tutorials*, vol. 20, no. 2, pp. 1329–1360, 2018.

[3] B. Clerckx, R. Zhang, R. Schober, D. W. K. Ng, D. I. Kim, and H. V. Poor, "Fundamentals of Wireless Information and Power Transfer: From RF Energy Harvester Models to Signal and System Designs," *IEEE Journal on Selected Areas in Communications*, vol. 37, no. 1, pp. 4–33, Jan. 2019.

[4] X. Lu, P. Wang, D. Niyato, D. I. Kim, and Z. Han, "Wireless Networks With RF Energy Harvesting: A Contemporary Survey," *IEEE Communications Surveys & Tutorials*, vol. 17, no. 2, pp. 757–789, 2015.

[5] Z. Ding et al., "Application of smart antenna technologies in simultaneous wireless information and power transfer," *IEEE Communications Magazine*, vol. 53, no. 4, pp. 86–93, Apr. 2015.

[6] B. Clerckx, K. Huang, L. Varshney, S. Ulukus, and M. Alouini, "Wireless Power Transfer for Future Networks: Signal Processing, Machine Learning, Computing, and Sensing," *IEEE Journal of Selected Topics in Signal Processing*, vol. 15, no. 5, pp. 1060–1094, Aug. 2021.

[7] K. Pattamasiriwat and C. Jaikaeo, "Distributed Region-Based Monitoring in Low-Power Listening Wireless Sensor Networks", *ECTI Transactions on Computer and Information Technology*, vol. 16, no. 1, pp. 21–34, Feb. 2022.

[8] Q. Wu and R. Zhang, "Towards Smart and Reconfigurable Environment: Intelligent Reflecting Surface Aided Wireless Network," *IEEE Communications Magazine*, vol. 58, no. 1, pp. 106–112, Jan. 2020.

[9] Q. Wu, S. Zhang, B. Zheng, C. You, and R. Zhang, "Intelligent reflecting surface-aided wireless communications: a tutorial," *IEEE Trans. Commun.*, vol. 69, no. 5, pp. 3313–3351, Jan. 2021.

[10] S. Gong, X. Lu, D. T. Hoang, D. Niyato, L. Shu, D. I. Kim, and Y. C. Liang, "Towards smart wireless communications via intelligent reflecting surfaces: A contemporary survey," *IEEE Commun. Surv. Tut.*, vol. 22, no. 4, pp. 2283–2314, Jun. 2020.

[11] M. Di Renzo, A. Zappone, M. Debbah, M. S. Alouini, C. Yuen, J. de Rosny, and S. Tretyakov, "Smart radio environments empowered by reconfigurable intelligent surfaces: How it works, state of research, and the road ahead," *IEEE J. Sel. Areas Commun.*, vol. 38, no. 11, pp. 2450–2525, Jul. 2020.

[12] C. Pan, H. Ren, K. Wang, J. F. Kolb, M. Elkashlan, M. Chen, M. Di Renzo, Y. Hao, J. Wang, A. L. Swindlehurst, X. You, and L. Hanzo, "Reconfigurable intelligent surfaces for 6G systems: Principles, applications, and research directions," *IEEE Commun. Mag.*, vol. 59, no. 6, pp. 14–20, Jul. 2021.

[13] E. Basar, M. Di Renzo, J. De Rosny, M. Debbah, M. S. Alouini, and R. Zhang, "Wireless communications through reconfigurable intelligent surfaces," *IEEE Access*, vol. 7, pp. 116753–116773, Aug. 2019.

[14] Q. Wu and R. Zhang, "Weighted sum power maximization for intelligent reflecting surface aided SWIPT," *IEEE Wireless Commun. Lett.*, vol. 9, no. 5, pp. 586–590, May 2020.

[15] C. He, X. Xie, K. Yang, and Z. J. Wang, "A Joint Power Splitting, Active and Passive Beamforming Optimization Framework for IRS Assisted MIMO SWIPT System," *arXiv preprint arXiv:2105.14545*, May 2021.

[16] J. Xu, Z. Zhong, and B. Ai, "Wireless powered sensor networks: Collaborative energy beamforming considering sensing and circuit power consumption," *IEEE Wireless Commun. Lett.*, vol. 5, no. 4, pp. 344–347, Aug. 2016.

[17] Z. Wang, Y. Shi, Y. Zhou, H. Zhou, and N. Zhang, "Wireless-powered over-the-air computation in intelligent reflecting surface-aided iot networks," *IEEE Internet Things J.*, vol. 8, no. 3, pp. 1585–1598, Aug. 2020.

[18] Z. Feng, B. Clerckx, and Y. Zhao, "Waveform and beamforming design for intelligent reflecting surface aided wireless power transfer: Single-user and multi-user solutions," *IEEE Trans. on Wireless Commun.*, vol. 21, no. 7, pp. 5346– 5361, Jul. 2022.

[19] Y. Zheng, S. Bi, Y. J. A. Zhang, X. Lin, and H. Wang, "Joint beamforming and power control for throughput maximization in IRS-assisted MISO WPCNs," *IEEE Internet Things J.*, vol. 8, no. 10, pp. 8399–8410, Dec. 2020.

[20] B. Ozpoyraz, A. T. Dogukan, Y. Gevez, U. Altun, E. Basar,"Deep learning-aided 6G wireless networks: A comprehensive survey of revolutionary PHY architectures," *arXiv preprint arXiv:2201.03866*, Jan. 2022.

[21] K.M. Faisal and W. Choi, "Machine Learning Approaches for Reconfigurable Intelligent Surfaces: A Survey," *IEEE Access*, vol. 10, pp.27343–27367, Mar. 2022.

[22] H. Sun, X. Chen, Q. Shi, M. Hong, X. Fu, and N. D. Sidiropoulos, "Learning to optimize: Training deep neural networks for wireless resource management," *IEEE Trans. Signal Process.*, vol. 66, no. 20, pp. 5438–5453, Oct. 2018

[23] W. Lee, O. Jo, and M. Kim, "Intelligent resource allocation in wireless communications systems," *IEEE Commun. Mag.*, vol. 58, no. 1, pp. 100–105, Jan. 2020.

[24] O. Ozdogan and E. Bjornson, "Deep learning-based phase reconfiguration for intelligent reflecting surfaces," in *Proc. IEEE Int. Conf. Acoust., Speech, Signal Process.*(ICASSP), Barcelona, Spain, May 2020, pp. 9160–9164.

[25] B. Sheen, J. Yang, X. Feng, and M. M. U. Chowdhury, "A deep learning based modeling of reconfigurable intelligent surface assisted wireless communications for phase shift configuration," *IEEE Open J. Commun. Soc.*, vol. 2, pp. 262–272, Jan. 2021.

[26] T. Lin and Y. Zhu, "Beamforming design for large-scale antenna arrays using deep learning," *IEEE Wireless Commun. Lett.*, vol. 9, no. 1, pp. 103–107, Sep. 2020.

[27] J. Gao, C. Zhong, X. Chen, H. Lin, and Z. Zhang, "Unsupervised learning for passive beamforming," *IEEE Commun. Lett.*, vol. 24, no. 5, pp. 1052–1056, Jan. 2020.

[28] H. T. Thien, P. V. Tuan, and I. Koo, "A secure-transmission maximization scheme for SWIPT systems assisted by an intelligent reflecting surface and deep learning," *IEEE Access*, vol. 10, pp. 31851–31867, Mar. 2022.

[29] P. V. Tuan and P. N. Son, "Intelligent reflecting surface assisted transceiver design optimization in non-linear SWIPT network with heterogeneous users," *Wireless Networks*, pp. 1–20, Apr. 2022.

[30] Z. Q. Luo, W. K. Ma, A. M. C. So, Y. Ye, and S. Zhang, "Semidefinite relaxation of quadratic optimization problems," *IEEE Signal Process. Mag.*, vol. 27, no. 3, pp. 20–34, May 2010.

[31] S. Boyd, and L. Vandenberghe, *Convex Optimization*. Cambridge, UK, Cambridge university press, 2004.

[32] M. Grant and S. Boyd, "CVX: Matlab software for disciplined convex programming," 2016. [Online] Available: http://cvxr.com/cvx.

[33] Q. Wu and R. Zhang, "Joint active and passive beamforming optimization for intelligent reflecting surface assisted SWIPT under QoS constraints," *IEEE J. Sel. Areas Commun.*, vol. 38, no. 8, pp. 1735–1748, Jul. 2020.

[34] A. H. Phan, H. D. Tuan, H. H. Kha, and D. T. Ngo, "Nonsmooth optimization for efficient beamforming in cognitive radio multicast transmission," *IEEE Trans. Signal Process.*, vol. 60, no. 6, pp. 2941–2951, Mar. 2012.

[35] C.D. Meyer, *Matrix Analysis and Applied Linear Algebra*. Philadelphia, USA, Siam, 2000.

[36] C.Y. Chi, W.C. Li, and C.H. Lin, *Convex Optimization for Signal Processing and Communications*. Florida, USA, CRC press, 2017.

[37] S. Bi, C. K. Ho, and R. Zhang, "Wireless powered communication: Opportunities and challenges," *IEEE Commun. Mag.*, vol. 53, no. 4, pp. 117–125, Apr. 2015.

[38] Q. Wu, X. Guan, and R. Zhang, "Intelligent reflecting surface-aided wireless energy and information transmission: An overview." *Proceedings of the IEEE*, Nov. 2021.

[39] Y. Tang, G. Ma, H. Xie, J. Xu, and X. Han, "Joint Transmit and Reflective Beamforming Design for IRS-Assisted Multiuser MISO SWIPT Systems," *ICC 2020 - 2020 IEEE International Conference on Communications (ICC)*, Jun. 2020, pp. 1-6.

[40] Q. Wu and R. Zhang, "Intelligent reflecting surface enhanced wireless network: Joint active and passive beamforming design," in *Proc. IEEE Global Commun. Conf.* (GLOBECOM), Abu Dhabi, United Arab Emirates, Dec. 2018, pp. 1–6.

[41] D. P. Kingma and J. Ba, "Adam: A method for stochastic optimization," *arXiv preprint arXiv:1412.6980*, Dec. 2014.

Pham Viet Tuan received the B.E. degree (2005), M.E. degree (2011) in Electronics and Telecommunications Engineering from Ho Chi Minh City University of Technology, Vietnam, and Ph.D degree (2018) in Electrical and Computer Engineering from University of Ulsan, South Korea. He was as Postdoctoral Researcher at the Multimedia Communications System Laboratory, University of Ulsan, South Korea (2019). His research interests include optimizations, machine learning, SWIPT networks, and intelligent reflecting surface.

Vinh Anh Nghiem Quan received his Bachelor's Degree (2009) in Computer Science from Hue University of Education, Vietnam and Master's Degree in Computer Science at University Laval, Canada. He currently works a lecturer and researcher at Hue University of Education. His fields of interests include machine learning, natural language processing, and computer vision.

Pham Ngoc Son received the B.E. degree (2005) and M.Eng. degree (2009) in Electronics and Telecommunications Engineering from Post and Telecommunication Institute of Technology, Ho Chi Minh City and Ho Chi Minh City University of Technology, Vietnam, respectively. In 2015, he received the Ph.D. degree in Electrical Engineering from University of Ulsan, South Korea. He is currently a Lecturer in the Faculty of Electrical and Electronics Engineering of Ho Chi Minh City University of Technology and Education (HCMUTE). His major research interests are cooperative communication, cognitive radio, physical layer security, energy harvesting, non-orthogonal multiple access, intelligent reflecting surface and short packet communications.

Sang Quang Nguyen received the B.E. degree from Ho Chi Minh City University of Transport, Ho Chi Minh City, Vietnam, in 2010, the M.E. degree from Ho Chi Minh City University of Technology, Ho Chi Minh City, in 2013, and the Ph.D. degree in electrical engineering from the University of Ulsan, Ulsan, South Korea, in 2017. From January 2017 to June 2017, he was a Postdoctoral Research Fellow with Queen's University Belfast, Belfast, U.K. From June 2017 until May 2021, he has been a Lecturer with Duy Tan University, Ho Chi Minh City. Since May 2021, He is head of Science of International Cooperation Department, as well as a lecturer with Ho Chi Minh City University of Transport. His major research interests are: cooperative communication, cognitive radio network, physical layer security, energy harvesting, and non-orthogonal multiple access, artificial intelligence.

Pham Viet Hung received the B. Eng, M.Sc and Ph.D degree in Electronics and Telecommunications from Hanoi University of Science and Technology in 2003, 2007 and 2015, respectively. From 2003 until now he has been working at Faculty of Electric and Electronics, Vietnam Maritime University. He was as Postdoctoral Researcher at the Communication and Networking Laboratory, University of Ulsan, South Korea (2019). His research interests include signal processing in Global Navigation Satellite Systems, digital transmission, maritime communications and MIMO communications.